A MULTI-MODE BLADE DAMPING CONTROL USING SHUNTED PIEZOELECTRIC TRANSDUCERS WITH ACTIVE FEEDBACK STRUCTURE

The Structural Dynamics and Mechanics branch (RXS) is developing smart adaptive structures to improve fan blade damping at resonances using piezoelectric (PE) transducers. In this presentation, only one shunted PE transducer was used to demonstrate active control of multi-mode blade resonance damping on a titanium alloy (Ti-6Al-4V) flat plate model, regardless of bending, torsion, and 2-stripe modes. This work would have a significant impact on the conventional passive shunt damping world because the standard feedback control design tools can now be used to design and implement electric shunt for vibration control. In other words, the passive shunt circuit components using massive inductors and resistors for multi-mode resonance control can be replaced with digital codes. Furthermore, this active approach with multi patches can simultaneously control several modes in the engine operating range. Dr. Benjamin Choi presented the analytical and experimental results from this work at the Propulsion-Safety and Affordable Readiness (P-SAR) Conference in March, 2009. This work is supported by the Subsonic Fixed Wing (SFW) Project (Janet Hurst, Project Manager).

A Multi-Mode Blade Damping Control Using Shunted Piezoelectric Transducers with Active Feedback Structure

Benjamin Choi
and
Carlos Morrison, James Min
NASA Glenn Research Center, Cleveland, Ohio, 44135

with support from
Kirsten Duffy, Milind Bakhle, Jeffrey Trudell, and Andrew Provenza

Objective

To investigate possibility of using an active resonance controller for turbomachinery blade with piezoelectric patches.

Outline

I. Introduction
II. Passive shunt damping
III. Active feedback controller design and analysis
IV. Experimental test results
V. Summary

I. Introduction

Previous activities at GRC

- Developed new damping technologies to reduce excessive vibratory stresses that lead to high cycle fatigue (HCF) failures in aircraft engine turbomachinery.
- Investigated several damping methods such as viscoelastic damping (O. Mehmed with J. Kosmatka, UC San Diego), passive impact damper, plasma sprayed damping coating, and HTSMA (K. Duffy).

Current efforts at GRC

To develop a damping technology for fan blade incorporating smart structure vs. material such as piezoelectric (PE) materials or shape memory alloy (SMA).

- Shape memory alloy (SMA): blade stiffness change or shape change by electrical heating. Slow response to rotating/moving parts.
- Piezoelectric (PE) devices: change in peak amplitude at blade resonance by oscillating electric signal. Selected due to fast response to voltage/current signal from controller.
- Passive analog circuits are being tested under rotating environment (K. Duffy).

I. Introduction *(continued)*

Two conventional control approaches for PE blade damping

- Passive damping (or shunt damping): PE transducer is shunted by a **passive electric circuit** that acts as a medium for dissipating mechanical energy of the base structure – (Hagood and von Flotow, 1990). Since then, numerous references have been available.

- Typical feedback control: PE transducers are being used as actuators and sensors for vibration control of flexible structures. These materials strain when exposed to a voltage and conversely produce a voltage when strained. Thus, one can minimize unwanted vibrations to the base structure by applying a 180 out-of-phase voltage to the PE actuator. One of them is PD (proportional and derivative) controller.

Literature survey for recent advances

1. Shunted piezoelectric circuit for turbomachinery blades

- **Passive control of turbomachine blading flow-induced vibrations (C. Cross, 2002).**

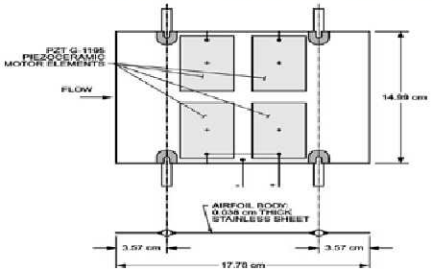

Flat plate airfoil with PE elements

- Passage perforated plates on the rotor was used to generate wake ➔ Then the PE stators were excited in a chordwise bending mode.
- A synthetic inductor (Chen, 1986) was produced to replace $L = 342\ H$ to control the ***first bending*** mode.

- **Passive shunt circuit was tested for piezoblade damping (S. Livet, 2008).**

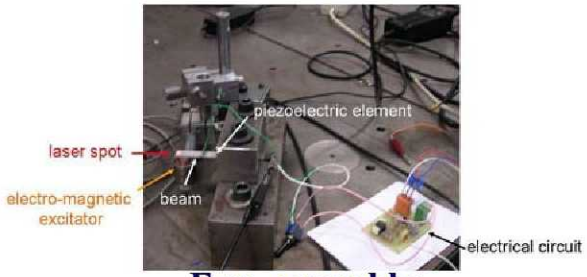

Exp. assembly

- Excited the blade by an electro-magnetic generator and damped by a virtual inductor (or gyrator) that consists of op amps, ext. power supply, resistors and capacitors.

- **Numerous papers published for passive control for rotorcraft vibration.**

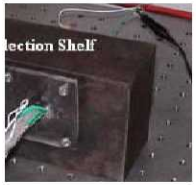

- Demonstrated a variety of passive techniques using PE transducer at the test lab. To authors' best knowledge, none of them showed the actual demonstration on the rotating blades.

2. Active control of PE actuator for turbomachinery blades

- **Cascade flutter control using PE device in subsonic flow.**
  (T. Watanabe, 2005, under NASA Quiet Engine Program)

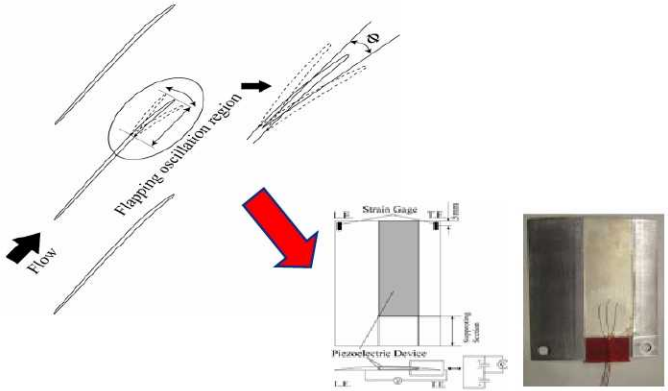

- Passage shock wave was generated at the trail edge of airfoil ➔ Induced unsteady aerodynamic work, causing instability.
- Trailing edge of airfoil was oscillated by P.E. to control the passage shock.

- **Low-speed fan noise control using PE actuators mounted on stator vanes:**
  (P. Remington, 2003)

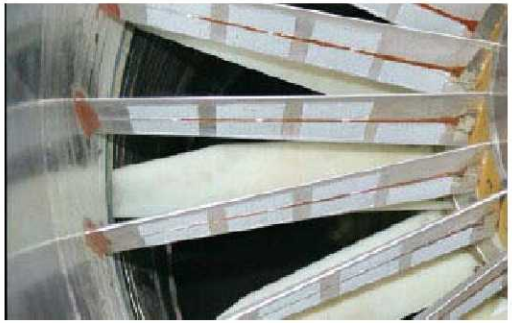

Actuators installed in the Stator Vanes.

- 210 vane actuators in the stator vanes of the Active Noise Control Fan (ANCF) test rig were tested to control fan-stator interaction noise. Good noise reductions achieved.

Active control of PE actuator for turbomachinery blades *(continued)*

- **Active control was tested for piezoblade damping (S. Livet, 2007).**

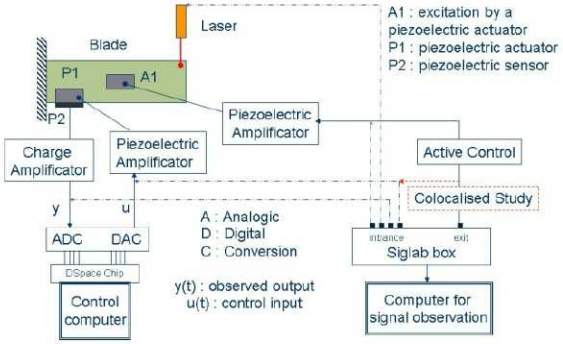

Experimental active control protocol

- Used a typical active control law (PD control) and achieved $\zeta = 0.9\%$.

- **In collaboration with Boeing, NASA developing shape-shifting helicopter blades (2009).**

Full-scale helicopter smart blade in a Ames Res. Ctr. wind tunnel

- When active control voltage is applied, blades extend a small amount, creating a mechanical motion that moves a flap up and down.
- Power transfer technique to the PE actuators in the rotating frame can benefits GRC's active blade damping research.

Summary of literature survey

- Room temperature PE patches were used for the stationary blades, not for the rotating blades yet.
- No pure passive circuit was used because of huge and messy inductor size. Instead semi-passive circuits were used to simulate physical inductors.
- For active damping cases, PD control law was used, which cannot make feedback effective at resonant frequencies.
- Wider and thicker patches were used, possibly resulting in aerodynamic performance penalty.

Our unique approach

- Extend to 1) rotating blades and 2) high temperatures. Need adaptive capability to change in eigen frequencies and nonlinear material properties.
- Implement pure passive circuits with $L_i \approx 0.89\,H$ on the rotating fan blade to suppress the resonant peaks at 3B and 2-stripe modes (K. Duffy).

- ***In this presentation***, we will demonstrate a passive shunt circuit with active feedback control architecture to reduce resonant peaks only. Passive circuits and adaptive feature can be easily programmable into a digital control code.
- Active shunt performances will be compared with conventional PD control performances in terms of peaks reduction and power consumption.

II. Passive Shunt Damping

Resistive/Inductive shunt

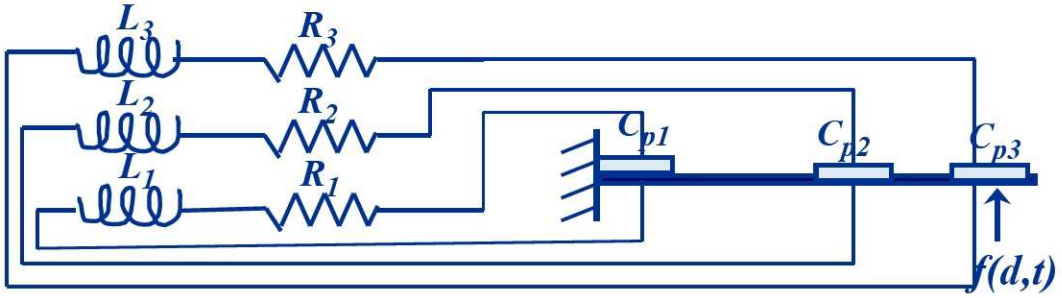

The electrical resonance frequency for i_{th} mode is

$$\omega_i = \frac{1}{\sqrt{L_i C}}$$

Ti 6A1-4V test plate	PE (QP10w)
E = 15.2*1e6; 15.2 Mpsi,	E_p = 1.03e7 psi
t_b = 0.078 in, thickness	t_a = 0.015 in, thickness
L = 8 in, length	L_p = 2 in, length
ρ = 0.16 lb/in^3, linear mass density	d_{31} = -60e-12, electric charge constant of PE
w_b = 3.2 in, width	w_p = 1.5 in, width
	k_{31} = 0.30, electro-mechanical coupling factor
	g_{31} = -15e-3, voltage constant
	c_{cap} = 60e-9, nF

Material properties and dimension of test specimen.

Target modes	L_i
2nd torsion mode at 625 Hz	1.082 H
3rd bending mode at 691 Hz	0.885 H
2-stripe mode at 1637 Hz	0.158 H

Serial shunt circuit inductor size for resonant damping.

II. Passive shunt damping *(continued)*

Passive controller implementation issues


+

+


$\approx 0.89\ H$ *for* ω_3

i_{th} mode circuit for multi-patches

x # of blades

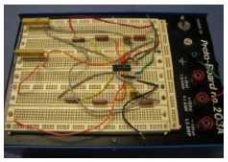

\+ Power supply

Semi-passive circuit

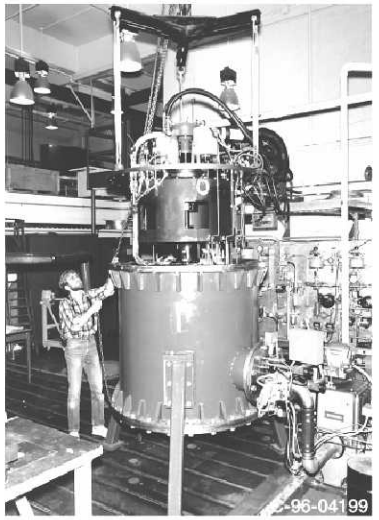

Dynamic Spin Rig

- Required huge inductor size mass to get a well tuned damping circuit.
- Rotor imbalance, electronic parts at high centrifugal loads /g-loads, installation space problem for multi-patches situation.
- Semi-passive circuit also required constant power supply. To resolve this problem, in collaboration with a company, a non-contact, inductively generated DC power transmitter is under development.
- Seems to be not practical in reality for the rotating blade.

III. Feedback Controller Design and Analysis

In 2003, Moheimani investigated similarities between the shunt damping systems and collocated active vibration controllers (S. Moheimani, 2003).

Digital control approach emulating passive circuit components

- Passive circuits can be easily **programmable** showing the shunted PE transducers can be viewed as a feedback control problem.
- Like a shunt circuit, the feedback is **effective only** at resonant frequencies.
- Also the active controller uses only one actuator to damp **several** of the blade's resonant modes regardless of bending, torsion and 2-stripe modes.

Digital controller implementation issues

- Operational overhead of transducing high voltage power to blade across slip ring. A telemetry system with a high power transmitting capability to the rotating blades is under development in collaboration with a company in order to replace the current slip ring of GRC's Dynamic Spin Rig.
- Potential cross talk between high voltage control signals to on blade sensors.
- Might encounter other unexpected problems.

Transfer function of analog *RLC* circuit

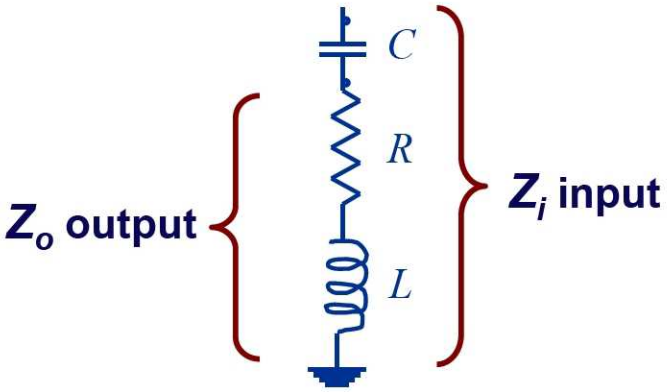

General feedback control *RLC* network.

$$Z_i = R + i\omega L - i/(\omega C)$$

$$Z_o = R + i\omega L$$

$$\frac{V_o}{V_i} = \frac{Z_o}{Z_i}$$

$$= \frac{R + i\omega L}{R + i\omega L - i/(\omega C)}$$

$$= \frac{Cs(R + Ls)}{LCs^2 + CRs + 1}$$

The controller is expressed in terms of passive circuit components (***LCR***) regardless of resonance types.

PID (proportional-integral-derivative) control law:

$$u(t) = MV(t) = K_p e(t) + K_i \int_0^t e(\tau)\,d\tau + K_d \frac{de}{dt}(t)$$

K_p: proportional gain, K_d: derivative gain

III. Feedback Controller Design/Analysis *(continued)*

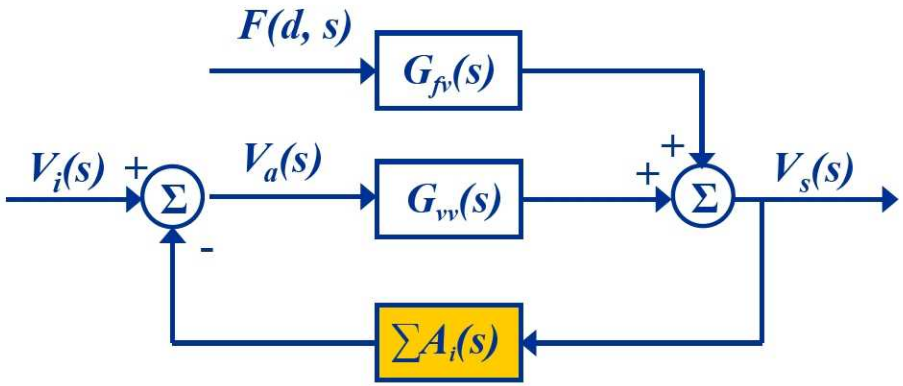

Feedback control block diagram for blade structure with PE.

The actuator voltage $V_a(s)$ is

$$V_a(s) = -A_i(s)V_s(s) + V_i(s)$$

where $A_i(s)$ is

$$A_i(s) = \frac{Cs(R + L_i s)}{L_i C s^2 + CR_i s + 1}$$

➢ A set of control laws in parallel circuits can be summed to control for several modes (B. Choi, 2008).

The closed-loop transfer functions

$$V_s(s) = \frac{G_{fv}(s)F(d,s)}{1 + A(s)G_{vv}(s)} + \frac{G_{vv}(s)V_i(s)}{1 + A(s)G_{vv}(s)}$$

$$Y(r,s) = \frac{G_{fy}(r,s)F(d,s)}{1 + A(s)G_{vv}(s)} + \frac{G_{vy}(r,s)V_i(s)}{1 + A(s)G_{vv}(s)}$$

where

$$G_{fv}(s) = \frac{V_a(s)}{F(d,s)}, G_{vv}(s) = \frac{V_s(s)}{V_a(s)}$$

$$G_{fy}(r,s) = \frac{Y(r,s)}{F(d,s)}, G_{vy}(s) = \frac{Y(r,s)}{V_a(s)}$$

III. Feedback Controller Design/Analysis *(continued)*

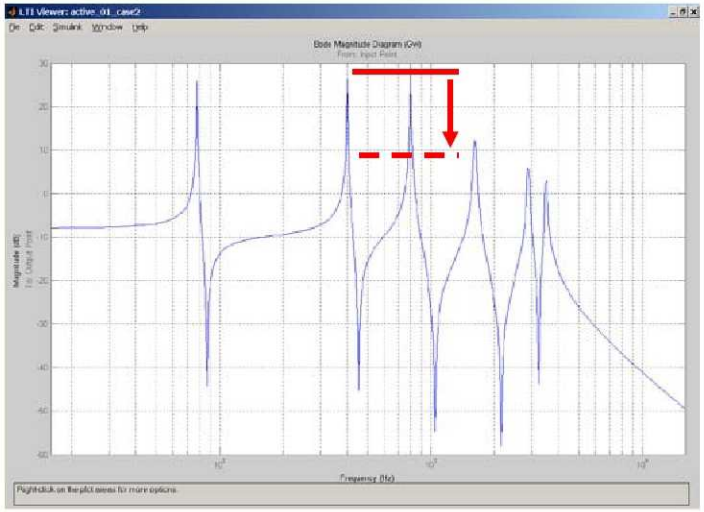

Analytical frequency response of G_{vv}

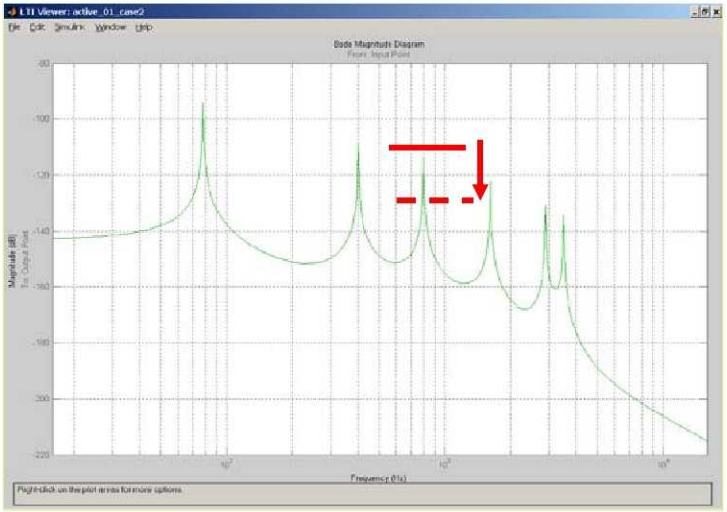

Analytical frequency response of G_{vy}

- Controller has to push peaks down to meet the design specification required for blade damping at resonances.
- Similarly, the transfer functions G_{fv} and G_{fy} can be obtained to complete a theoretical model of the laminated beam.

III. Feedback Controller Design/Analysis *(continued)*

Analytical open- and closed-loop frequency responses for multi-resonant damping.

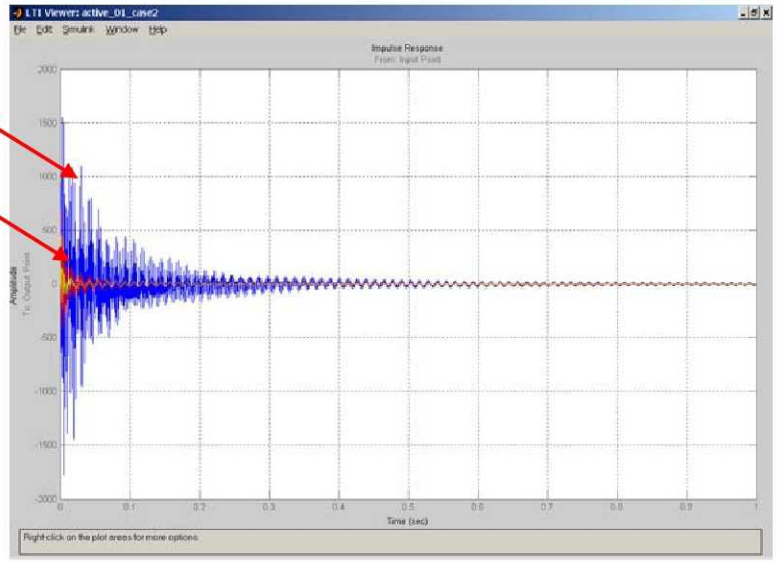

Impulse responses for open- and closed-loop system.

- This method can damp multiple resonance modes using one sensor-actuator pair.
- However, the control effort is very high because the PE patch was located very close to the root side (worst location) and the 1st bending mode included.
- Optimization process might be needed for an optimal control effort given performance requirement at each mode and existing control hardware capacity.

IV. Experimental Test Results

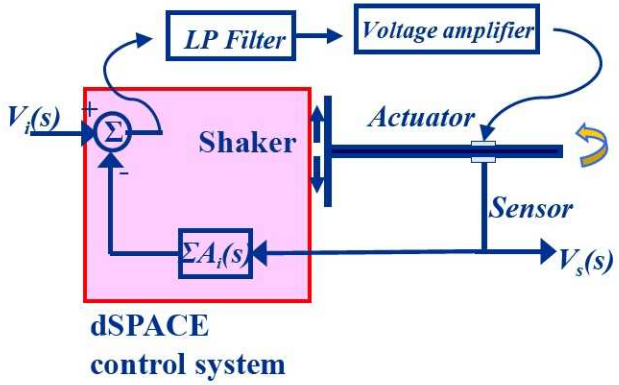

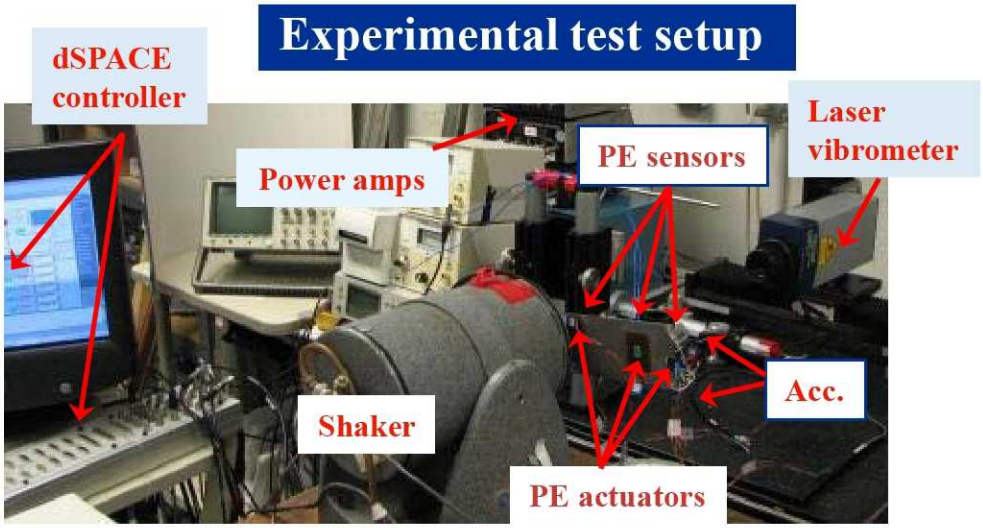

Flat plate: 8″×3.2″×.078″, PE wafer: 1.81″×1.31″×.010″

- Three PE patches for actuation and another three PE patches for sensing are bonded at the optimal locations for the target resonances – 3rd bending, 2 torsion, and 2-stripe modes at this demo.
- After fine-tuning the controller to the experimental target resonances, download the control algorithm to the dSPACE control system.
- HP Analyzer generates swept sine signal to send to the shaker, and it reads all signals from accelerometers, PE sensors and actuators, and controller voltages and currents from the power amplifiers.
- We analyze closed-loop and open-loop transfer functions to investigate achieved damping performance for the target modes.

IV. Experimental Test Results (*continued*)

1). 3rd Bending Control

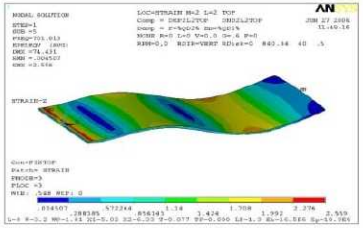

Optimal location

a).

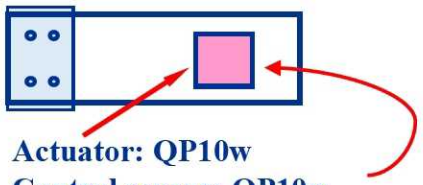

Non-optimal location

b).

2). 2nd Torsion Control

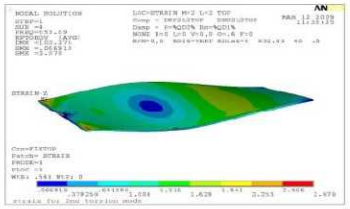

a).

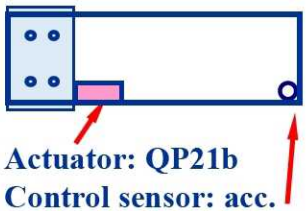

b).

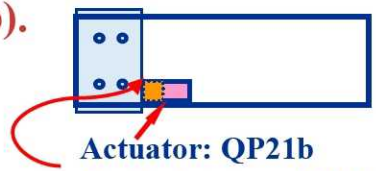

3). 2-Stripe Control

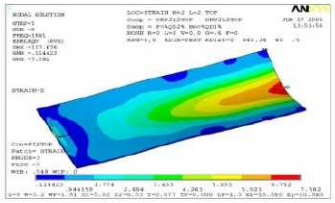

a).

b).

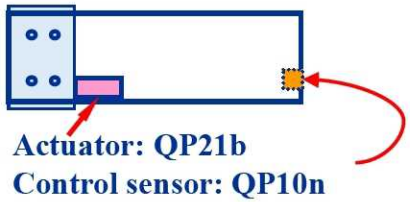

c).

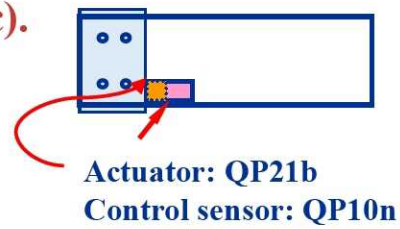

Notice that *only one* actuator was used.

IV. Experimental Test Results (*continued*)

1.a) 3rd Bending Mode Control

Active damping using optimally located 3B PE actuator and collocated identical PE sensor

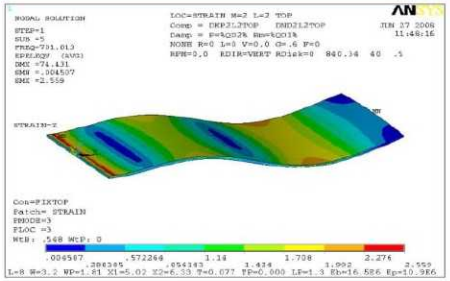

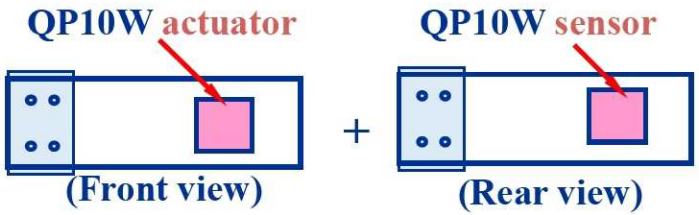

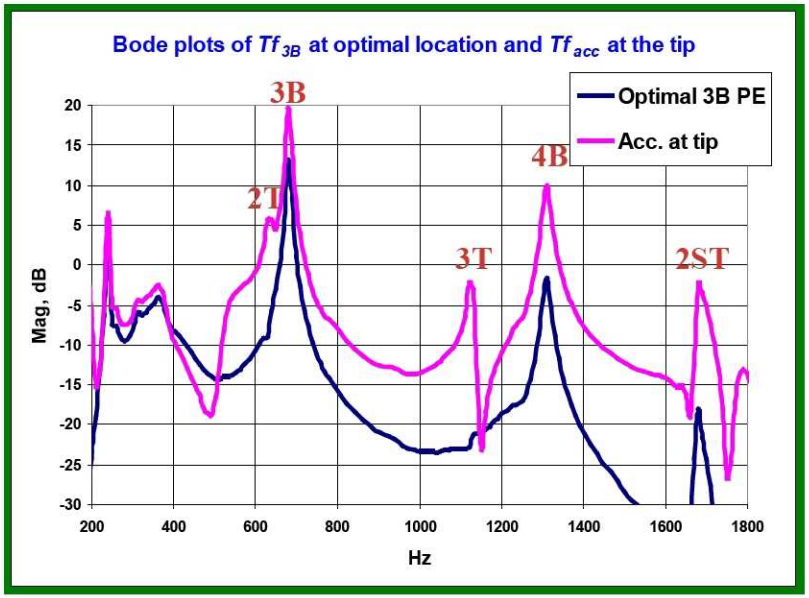

Exp. open-loop $T_f|3B/f_{base}|$ and $T_f|acc_{tip}/f_{base}|$. Our target resonances are 2T, 3B and 2-stipe modes.

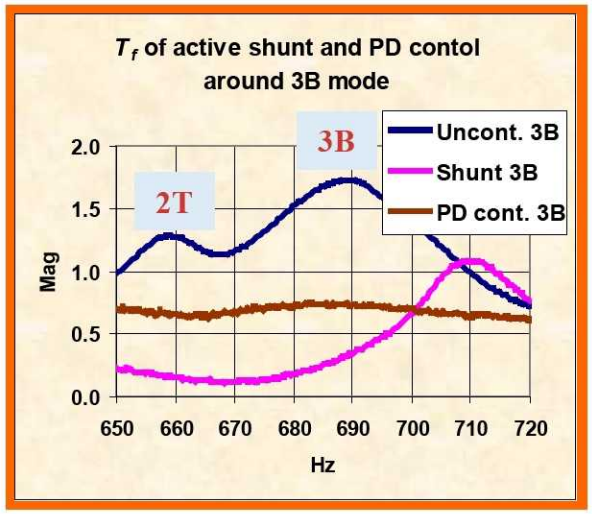

Exp. open- and closed-loop bode plots of Tf_{3B} around third bending mode. PD controller reduced neighborhood of 3B, while the shunt controller reduced 3B peak only. A little mistuned resonant controller shown here.

IV. Experimental Test Results (*continued*)

1.a) 3rd Bending Mode Control (*continued*)

Time history of Acc. and 3B disp. when base excitation force of 10mV*sin(691Hz*t) injected

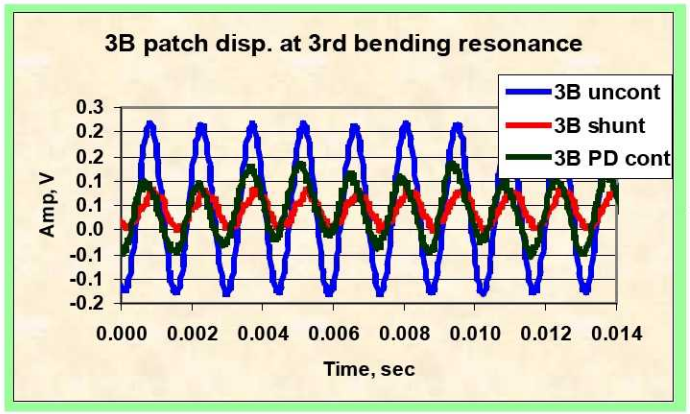

Active shunt reduced the peak by 78% and conventional PD controller reduced by 58%.

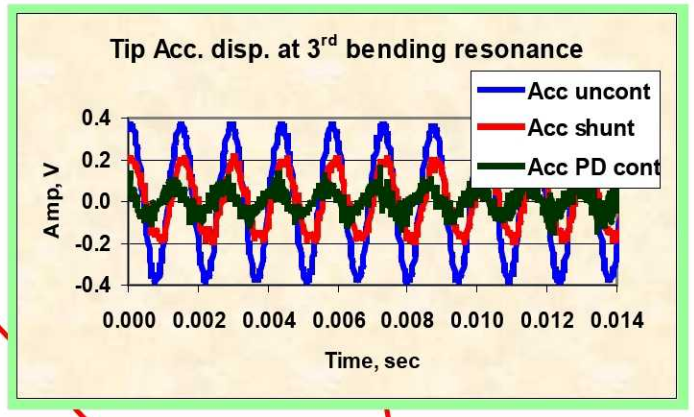

Active shunt reduced the peak by 48% and conventional PD controller reduced by 75%.

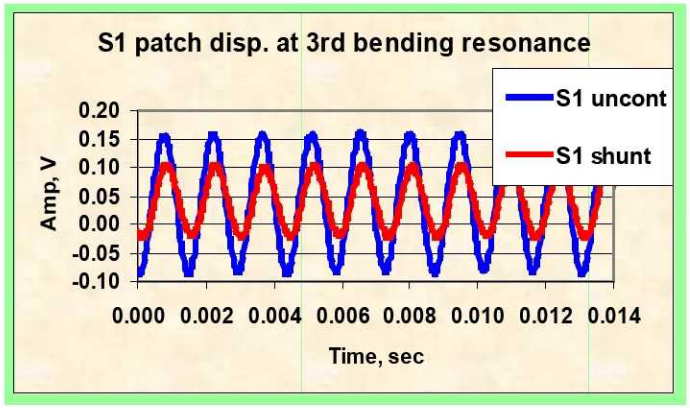

Active shunt reduced the peak by 58%.

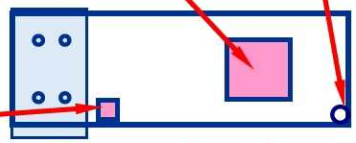

Sensors location

IV. Experimental Test Results (*continued*)

This movie shows the time history of controlled and uncontrolled tip displacement and strain level at the PZT location when the excitation force of 5mV*sin(691 Hz*t) was injected.

➔ **Please click the screen for the demo video.**

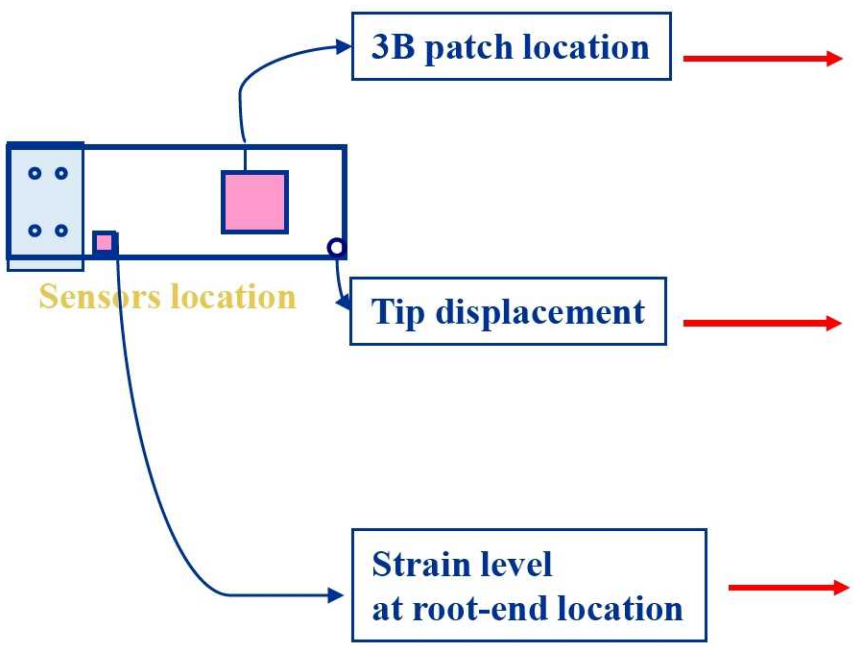

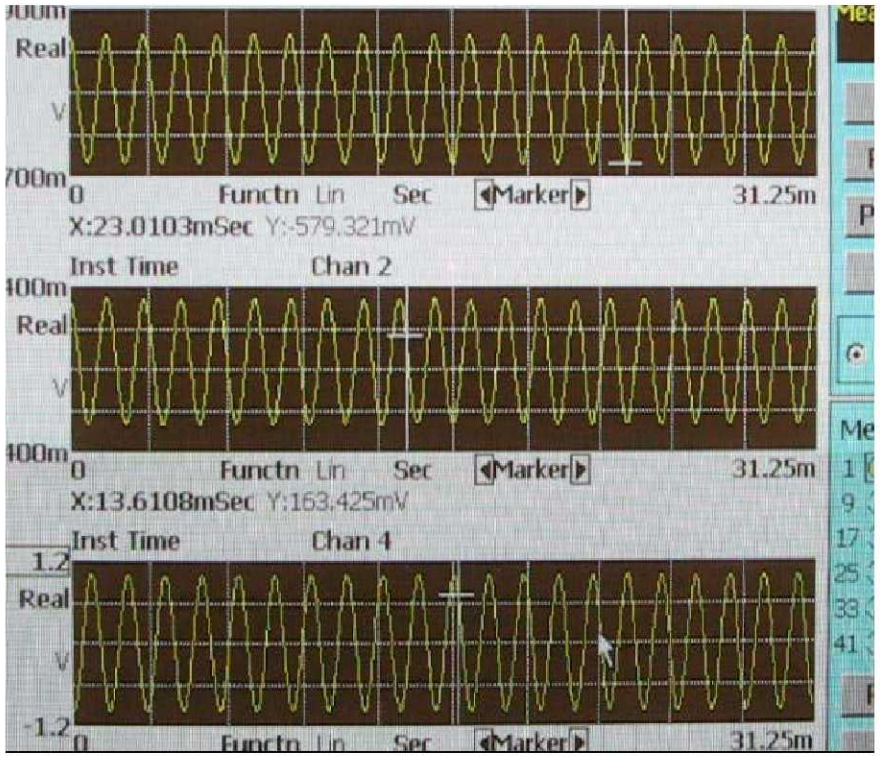

1.a) 3rd Bending Mode Control (*continued*)

Power comparison of active shunt and conventional PD controller:

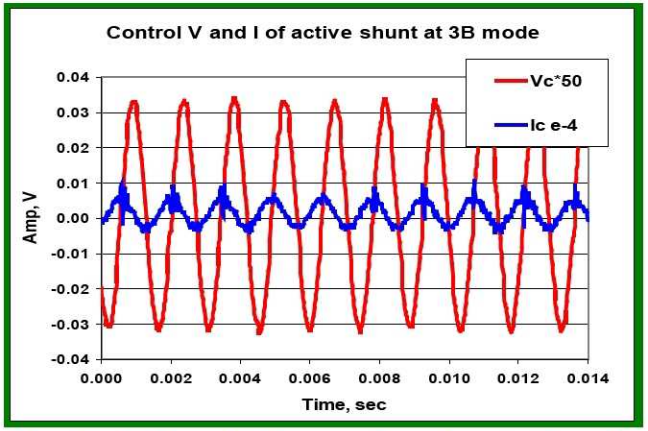

Control *V* and *I* for active shunt circuit.

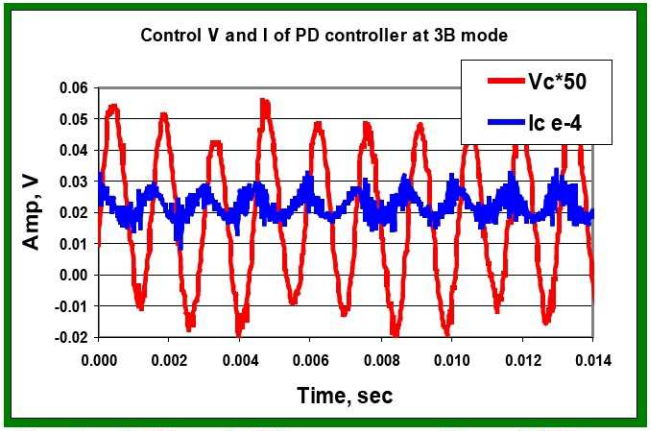

Control *V* and *I* for conventional PD controller.

- The average power over a complete cycle can be expressed as

$$P_{avg} = \frac{V_{peak}}{\sqrt{2}} \frac{I_{peak}}{\sqrt{2}} \cos\varphi$$

1) **Active shunt circuit:**

P_{avg} = 1.6 * 0.0041e-4 * *cos φ* *V-Amp*

≈ *0 W* even in phase (?)

2) **Conventional PD controller:**

P_{avg} = 1.5 * 0.0065e-4 * *cos φ* *V-Amp*

≈ *0 W* even in phase (?)

- Voltage signal for PD controller fluctuated while shunt control voltage signal was stable.
- For almost same performance, PD controller required 48% more power than active shunt circuit.

1.b) 3rd Bending Mode Control *(continued)*

Other approach using a non-optimal PE actuator and 3B PE sensor

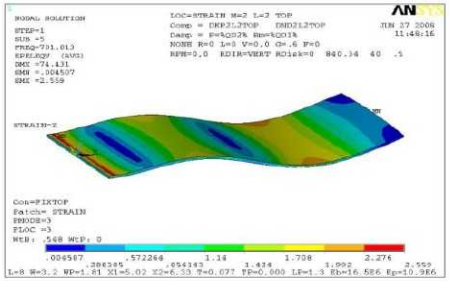

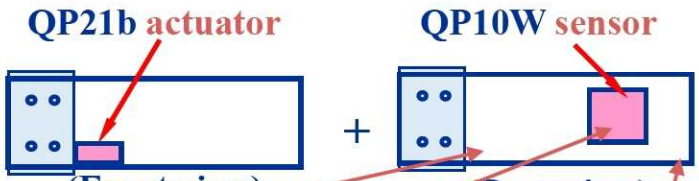

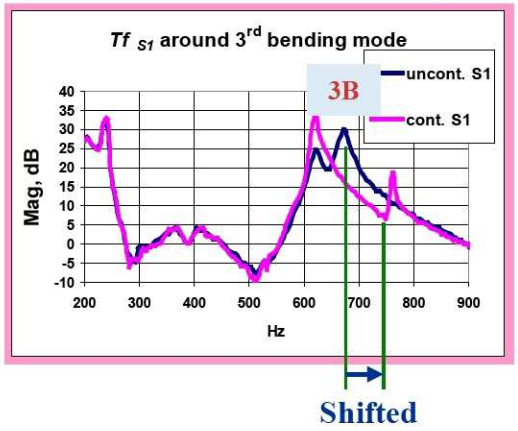

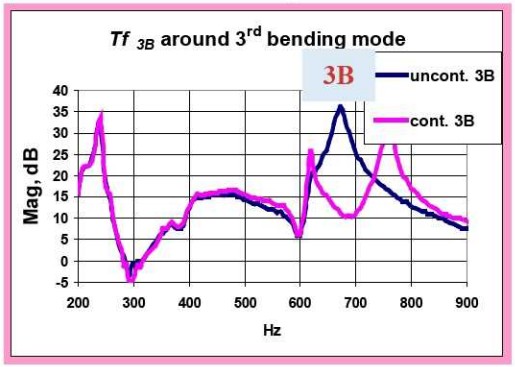

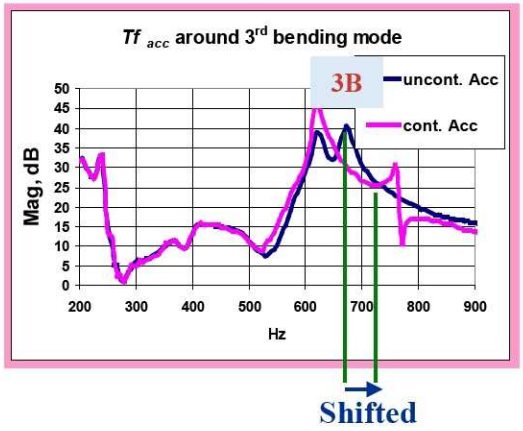

- Exp. bode plots of $Tf\,|S1/f_{base}|$, $Tf\,|3B/f_{base}|$, and $Tf\,|acc_{tip}/f_{base}|$. 3B location has about 84% peak reduction, but excessive damping caused drawback of two adjacent peaks.
- Shunted T_f of tip and root-end displacements were shifted right due to feedback gain and mainly mistuned resonant controller. To avoid this, calibration of glued PE's capacitance must be done to eliminate discrepancy between theoretical and exp. capacitor values.

1.b) 3rd Bending Mode Control *(continued)*

Time history of Acc. and 3B disp. when base excitation force of 10mV*sin(691Hz*t) injected

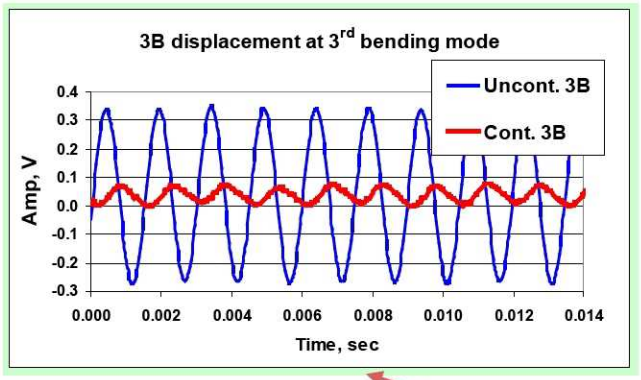

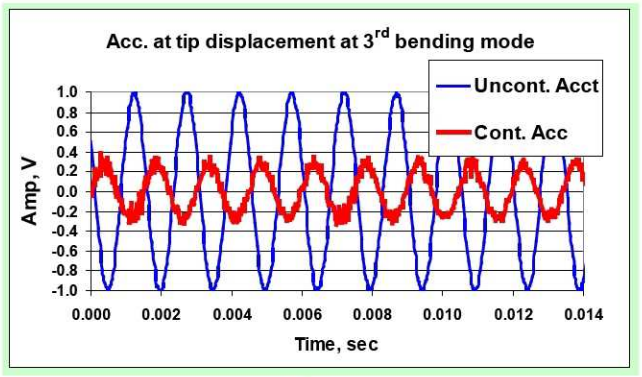

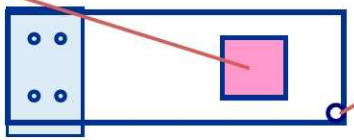

Sensors location

- Showed time history of controlled and uncontrolled displacements of blade tip and 3B location when the excitation force with 691 Hz was applied.
- More than **95%** reduction at the 3rd bending location on and **82%** of tip displacement (Acc) were achieved. Notice that only one small root-end actuator was used. If a pair of actuators used, the projected performance would have improved by a factor of 2 (?).

IV. Experimental Test Results (*continued*)

2.a) 2nd Torsion Mode Control

Active damping using optimal actuator and accelerometer to reduce the tip displacement

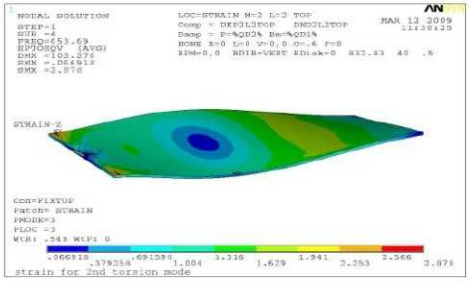

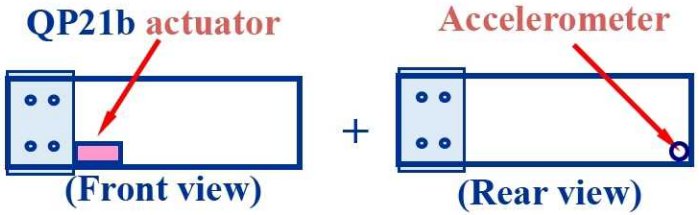

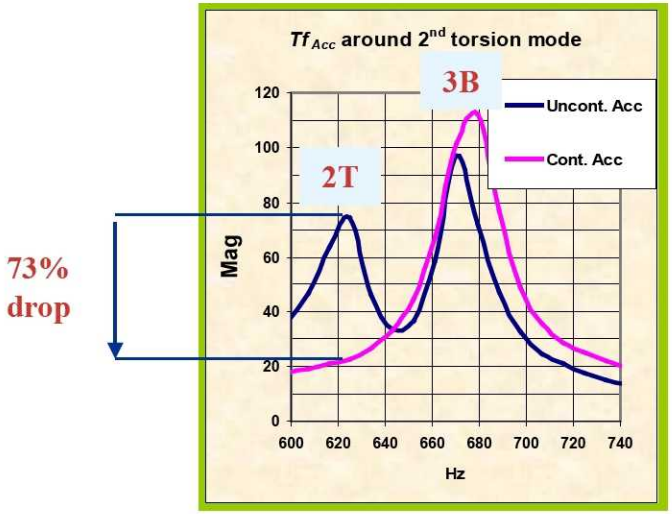

Exp. open- and closed-loop bode plots of Acc. at the tip.

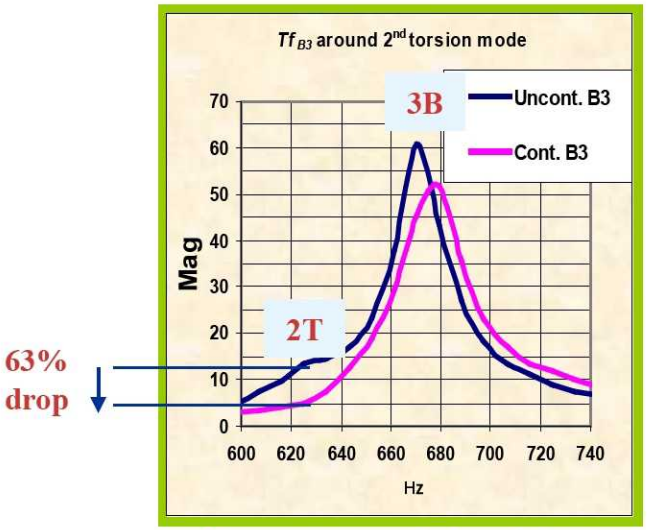

Exp. open- and closed-loop bode plots of 3B position.

- Accelerometer signal showed clear peak of 2nd torsion mode, while 3B position sensor barely showed 2nd torsion resonance peak as anticipated.

2.a) 2nd Torsion Mode Control (*continued*)

Time history of Acc. and 3B disp. when base excitation force of 10mV*sin(625Hz*t) injected

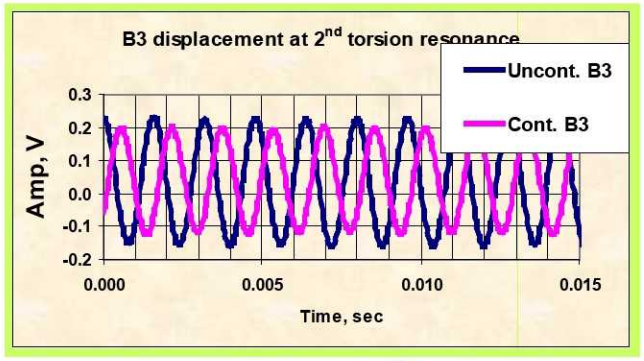

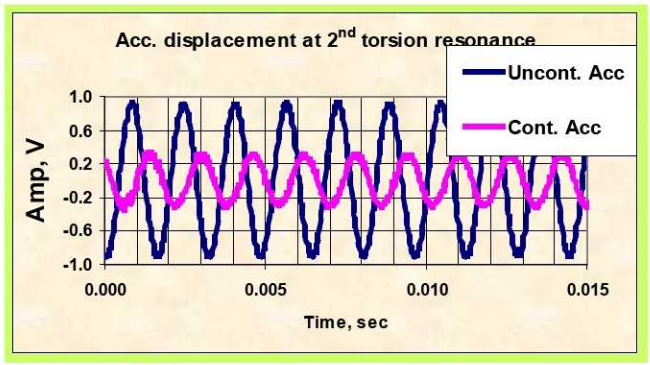

26% peak reduced.

69% peak reduced.

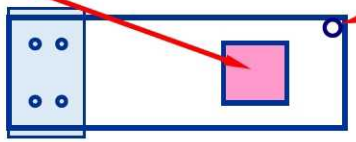

Sensors location

Power calculation:

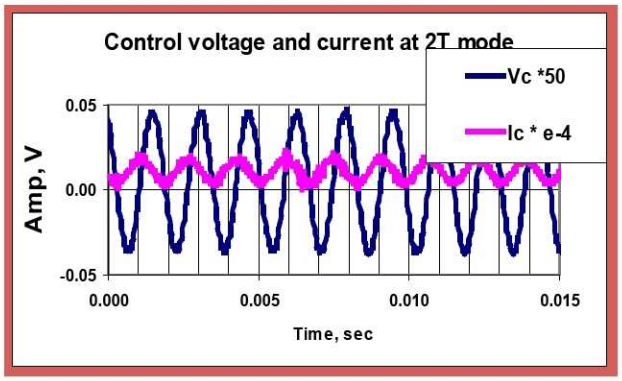

- The average power over a complete cycle can be expressed as

$$P_{avg} = \frac{V_{peak}}{\sqrt{2}} \frac{I_{peak}}{\sqrt{2}} \cos\varphi$$

P_{avg} = 14.2 * 0.0183e-4 * *cos φ* *V-Amp*

≈ *0 W* even in phase (?)

2.b) 2nd Torsion Mode Control (*continued*)

Active damping using optimal actuator and collocated sensor to reduce the strain level

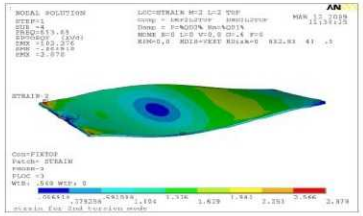

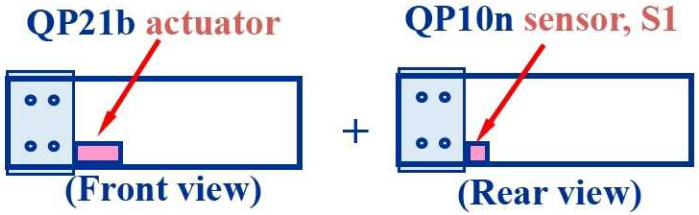

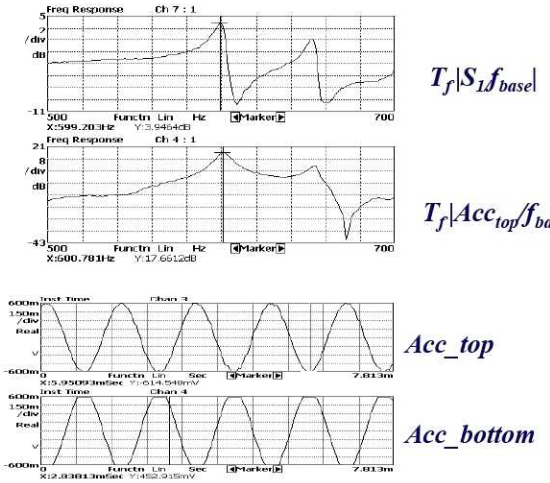

Exp. open-loop bode plot and time history of acc. signals.

Uncontrolled
S1: 3.95 dB
Tip: 17.7 dB

Controlled
S1: -6.84 dB
Tip: 11.6 dB

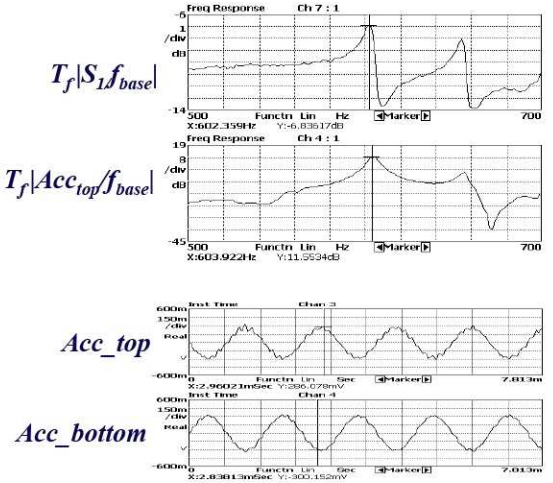

Exp. active shunt bode plot and time history of acc. signals.

- About **72%** reduction at the root-end sensor (S1) and **51%** reduction at the tip (Acc.) were achieved using ***only one set*** of actuator and sensor. Notice that two tip acc. signals are out of phase (180) due to the torsion mode.

IV. Experimental Test Results (*continued*)

3.a) 2-Stripe Mode Control

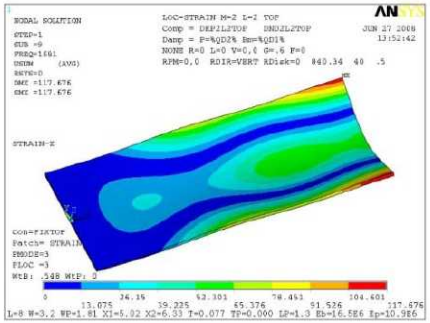

Optimal actuator and sensor to reduce the strain level

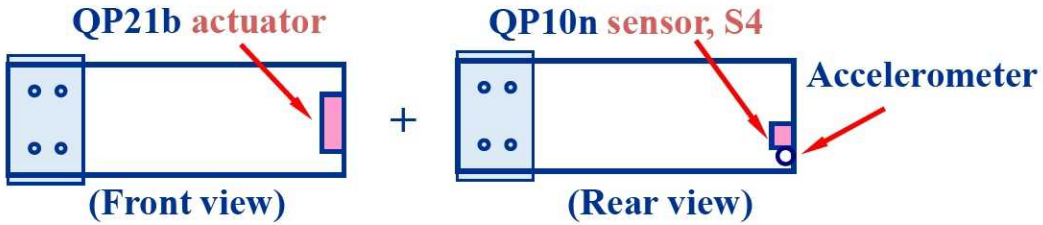

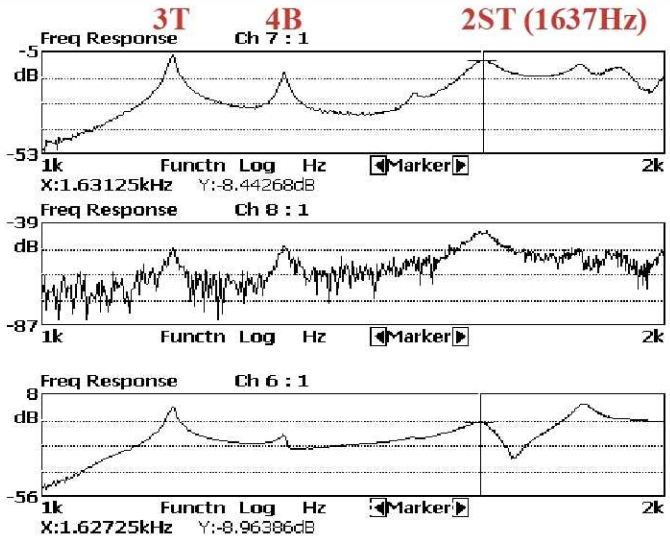

$T_f|Acc_{top}/f_{base}|$

$T_f|B_3/f_{base}|$

$T_f|Acc_{bot}/f_{base}|$

Exp. open-loop transfer function.

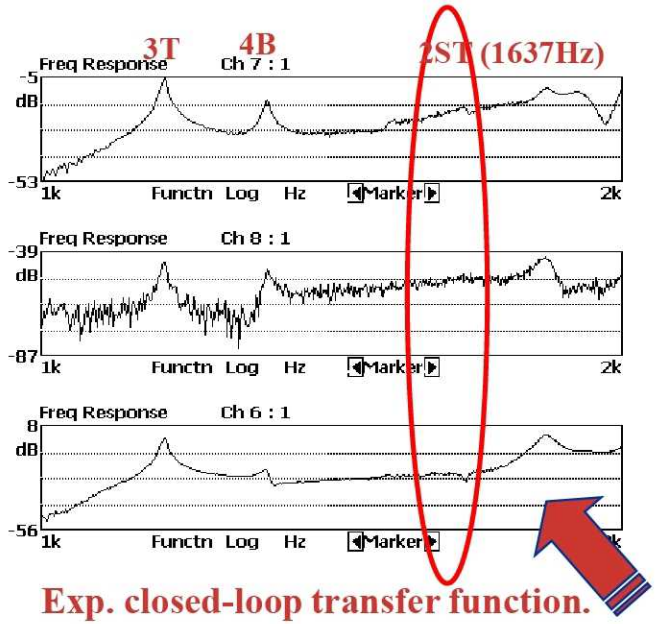

Exp. closed-loop transfer function.

- The peaks for the 2-stripe mode were gone.

3.a) 2-stripe Mode Control *(continued)*

Time history of sensor displacement when base excitation force of 10mV*sin(1637Hz*t) injected

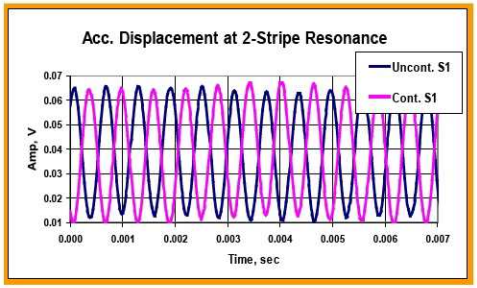

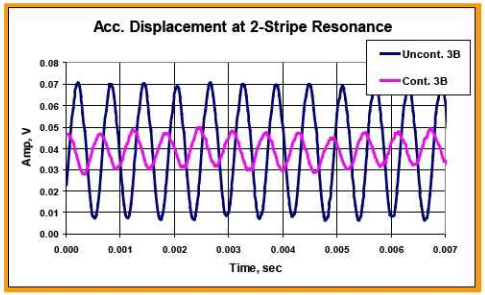

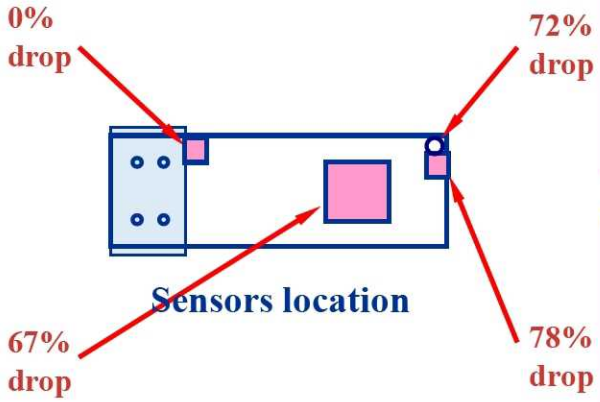

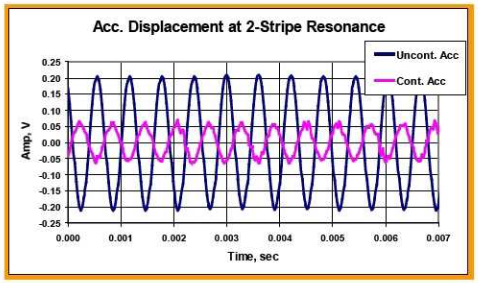

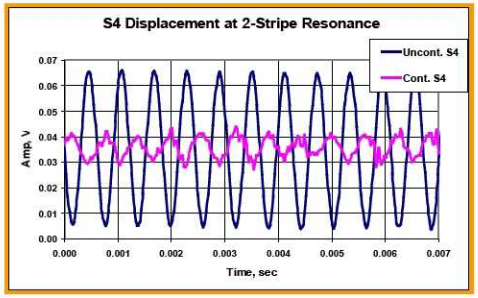

- Showed time history of controlled and uncontrolled tip, 3B location, root-end displacements when the excitation force with 1637 Hz was applied.
- As anticipated, more than **72%** reduction at the tip displacement (Acc and S4), **67%** reduction at the 3B location, and **0%** reduction in the root side position (S1) were achieved.

3.b) 3.c) 2-stripe Mode Control (*continued*)

Non-optimal actuator setup:

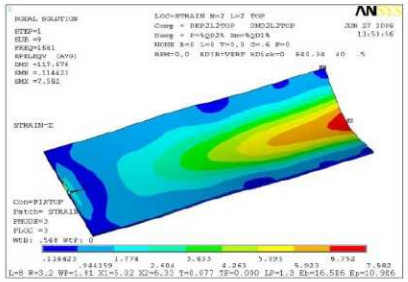

In this demo, a root-end actuator (not optimized location for 2-stripe mode control) and two different sensors (S4 and S1) were used to investigate how much resonance peak at the 2-stripe mode could be reduced.

3.b)

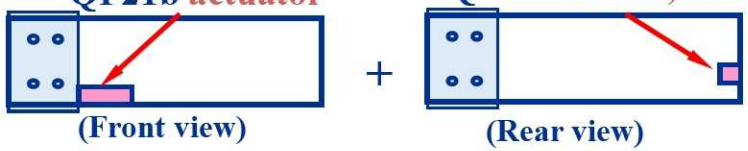

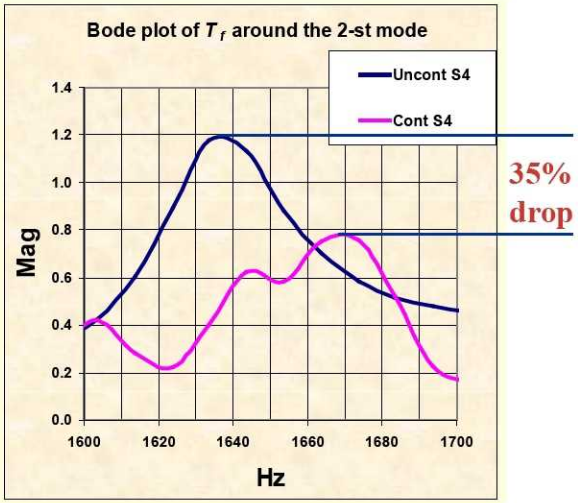

Exp. open- and closed-loop bode plots of S4.

3.c)

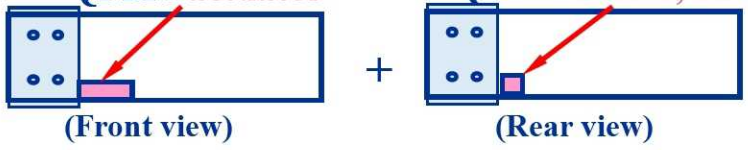

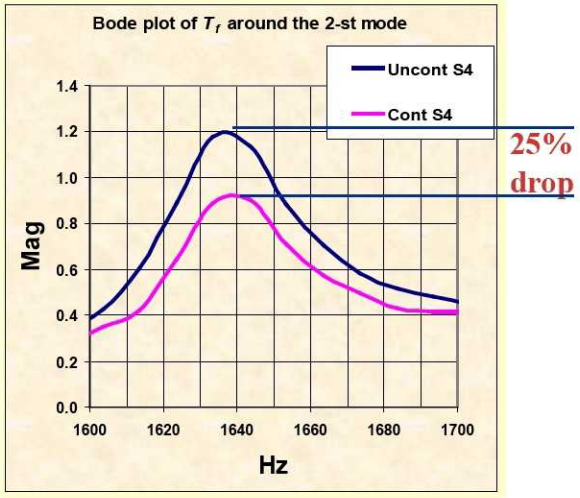

Exp. open- and closed-loop bode plots of S4.

V. Summary

- Demonstrated that a passive shunt circuit can be viewed as a feedback control problem and thus can be easily implemented into a programmable digital code. Easy to include adaptive features to the code.
- In other words, the passive shunt circuit components such as massive inductors and resistors for multimode resonance control can be replaced with a couple of lines in the code.
- This technique worked well to three target resonances, regardless of bending, torsion and 2-stripe modes.
- In collaboration with a company, GRC is developing a high power transferring device to actuate PE patches on the rotating frame.
- Further comprehensive research including a trade-off study must be done to demonstrate a viable means of using this approach for rotating blades through GRC's Dynamic Spin Rig test.